

# Demonstration of Chemical-Looping with Oxygen Uncoupling (CLOU) Process in a 1.5 kW<sub>th</sub> Continuously Operating Unit Using a Cu-based Oxygen-Carrier

Alberto Abad \*, Iñaki Adánez-Rubio, Pilar Gayán, Francisco García-Labiano, Luis F. de Diego, Juan Adánez

Instituto de Carboquímica (ICB-CSIC), Dept. of Energy & Environment, Miguel Luesma Castán, 4, Zaragoza, 50018, Spain

\*Corresponding author. Tel.: +34 976 733977; fax: +34 976 733318  
Email address: abad@icb.csic.es

## Abstract

Chemical-Looping with Oxygen Uncoupling (CLOU) process is a Chemical-Looping Combustion (CLC) technology that allows the combustion of solid fuels with inherent CO<sub>2</sub> separation. As in the CLC technology, in the CLOU process the oxygen necessary for the fuel combustion is supplied by a solid oxygen-carrier, which contains a metal oxide. The CLOU technology uses the property of the copper oxide which can generate gaseous oxygen at high temperatures. The oxygen generated by the oxygen-carrier reacts directly with the solid fuel, which is mixed with the oxygen-carrier in the fuel-reactor. The reduced oxygen-carrier is transported to the air-reactor where it is oxidized by air. The flue gases from the fuel-reactor are only CO<sub>2</sub> and H<sub>2</sub>O, since fuel is not mixed with air. This work demonstrates the proof of the concept of the CLOU technology burning coal in a 1.5 kW<sub>th</sub> continuously operated unit consisting of two interconnected fluidized-bed reactors. A bituminous coal was used as fuel. An oxygen-carrier prepared by spray drying containing 60 wt% CuO and MgAl<sub>2</sub>O<sub>4</sub> as supporting material was used as oxygen-carrier. The effects of fuel-reactor temperature, coal feeding rate, and solids circulation flow rate on the combustion and on the CO<sub>2</sub> capture efficiencies were investigated. Fast reaction rates of oxygen generation were observed with the oxygen-carrier and full combustion of coal was attained in the plant using a solids inventory  $\approx 235$  kg/MW<sub>th</sub> in the fuel-reactor. In addition, values close to 100 % in carbon capture efficiency were obtained at 960 °C. Results obtained are analyzed and discussed in order to be useful for the scale-up of a CLOU process fuelled with coal.

Keywords: CLOU, copper oxide, carbon capture, coal, combustion, CLC.

## 1. Introduction

According to the IPCC report on mitigation of climate change (IPCC, 2005), which considers different possible growing scenarios, Carbon Capture and Storage (CCS) would contribute with 15–55% to the cumulative mitigation effort worldwide until 2100 in order to stabilize CO<sub>2</sub> concentration in the atmosphere. CCS is a process involving the separation of CO<sub>2</sub> emitted by industry and energy-related sources, and its storage for isolation from the atmosphere over a long term. Chemical-Looping Combustion process (CLC) has been suggested among the best alternatives to reduce the economic cost of CO<sub>2</sub> capture using fuel gas (Kerr, 2005) and to reduce energy penalty compared with other CO<sub>2</sub> capture process (Kvamsdal et al., 2007). In this process, CO<sub>2</sub> is inherently separated from other combustion products, N<sub>2</sub> and unused O<sub>2</sub>, through the use of a solid oxygen-carrier and thus no energy is expended for its separation. A CLC system usually consists of two interconnected fluidized-bed reactors, designated as air-reactor and fuel-reactor, with the oxygen-carrier circulating between them. The CLC process has been demonstrated for gaseous fuel combustion such as natural gas and syngas in 10 to 140 kW<sub>th</sub> units using oxygen-carrier materials based on Ni (Linderholm et al., 2009; Kolbitsch et al., 2009), Cu (Adánez et al., 2006) and Fe (Lyngfelt et al., 2005; Pröll et al., 2009). All these oxygen-carriers have been reviewed by Adánez et al. (Adánez et al., 2011).

However, for energy generation is more relevant the use of the CLC concept for coal combustion because solid fuels are considerably more abundant and less expensive than natural gas. It would be highly advantageous if the CLC process could be adapted to coal, as well as other kind of solid fuels. First option to use solid fuels in a CLC process was to use syngas in the fuel-reactor coming from a previous gasifying step. However it is necessary to use pure oxygen for gasification of the solid fuel to apply this technology. This step has an important energy penalty due to the oxygen separation from the air. The second option of development is the Chemical-Looping Solid Fuel Combustion, where the solid fuel is directly introduced to the fuel-reactor which is fluidized by a gasifying agent, e. g. H<sub>2</sub>O or CO<sub>2</sub>. Because of the slow gasification reaction rate, a carbon stripper is necessary to separate the unreacted char particles from the oxygen-carrier, before it is regenerated with air, to avoid CO<sub>2</sub> emissions in this reactor (Berguerand and Lyngfelt, 2008; Cao and Pan, 2006). To increase the

gasification rate, temperatures higher than 1000 °C has been proposed to be used in the fuel-reactor (Berguerand and Lyngfelt, 2009). Moreover, there is a partial loss of oxygen-carrier in the purge stream of ash particles and low cost materials are preferred in this CLC option, e. g. ilmenite, hematite or anhidrite (Leion et al., 2008, 2009a; Shen et al., 2009; Wang and Anthony, 2008).

An alternative process, Chemical-Looping with Oxygen Uncoupling (CLOU), was recently proposed (Mattisson et al., 2009a) to overcome the low reactivity of the char gasification stage in the direct solid fuelled chemical-looping combustion. Mattisson and co-workers (Mattisson et al., 2009a) made use of the idea first proposed by Lewis and Gilliland (Lewis and Gilliland, 1954) to produce CO<sub>2</sub> from solid carbonaceous fuels by using gaseous oxygen produced by the decomposition of CuO.

Chemical-Looping with Oxygen Uncoupling (CLOU) process is based on the strategy of using oxygen-carrier materials which release gaseous oxygen in the fuel-reactor and thereby allowing the solid fuel to burn with gas phase oxygen. These materials can be also regenerated at high temperatures. In this way, the slow gasification step in the chemical-looping combustion with solid fuels is avoided, giving a much faster solid conversion (Mattisson et al., 2009b). In CLOU process, fluidization gas can be recycled CO<sub>2</sub>, reducing in this way the steam duty of the unit.

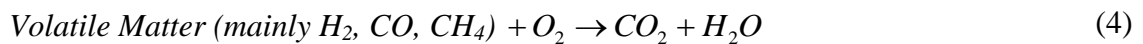
Fig. 1 shows a schematic diagram of a CLOU system. In the fuel-reactor CO<sub>2</sub> and H<sub>2</sub>O are produced by different reactions. First the oxygen-carrier releases oxygen according to:



and the solid fuel begins devolatilization producing a solid residue (char) and volatile matter as gas product :



Then, char and volatiles are burnt as in usual combustion according to reactions (3) and (4):



After steam condensation, a pure CO<sub>2</sub> stream can be obtained in the fuel-reactor. The reduced oxygen-carrier is transported to the air-reactor, where the oxygen-carrier is regenerated to the initial oxidation stage by reverse reaction (1) with the oxygen of the air, and being ready for a new cycle. The exit stream of the air-reactor contains only N<sub>2</sub> and unreacted O<sub>2</sub>. Therefore, CLOU process such as CLC technology has a low energy penalty for CO<sub>2</sub> separation and low CO<sub>2</sub> capture costs would be expected. The heat release over the fuel- and air-reactors is the same as for conventional combustion.

A special requirement is needed for the oxygen-carrier to be used in the CLOU process in comparison to oxygen-carriers for normal CLC, where the fuel must be able to react directly with the oxygen-carrier without any release of gas phase oxygen. Only those metal oxides that have a suitable equilibrium partial pressure of oxygen at temperatures of interest for combustion (800-1200 °C) can be used as CLOU oxygen-carriers for solid fuel combustion. CuO/Cu<sub>2</sub>O, Mn<sub>2</sub>O<sub>3</sub>/Mn<sub>3</sub>O<sub>4</sub>, and Co<sub>3</sub>O<sub>4</sub>/CoO have been identified as redox pairs with capacity to evolve oxygen at those temperatures (Mattisson et al., 2009a). Copper, manganese and cobalt oxides have an oxygen transport capacity of 10, 3 and 6.6 g O<sub>2</sub> per 100 g of metal oxide, respectively.

In the CLOU process, the O<sub>2</sub> release (reaction 1) must be reversible in order to oxidize the oxygen-carrier in the air-reactor and regenerate the material, which depends on the thermodynamic of the metal oxide used. Fig. 2 shows the partial pressure of oxygen as a function of the temperature for the systems CuO/Cu<sub>2</sub>O, Mn<sub>2</sub>O<sub>3</sub>/Mn<sub>3</sub>O<sub>4</sub>, and Co<sub>3</sub>O<sub>4</sub>/CoO, calculated using HSC software (HSC Chemistry 6.1, 2008). The respective reactions are endothermic for the three metal oxides, as it is showed in reactions (5), (6) and (7). Operating conditions in the air-reactor and fuel-reactor would come determined by the thermodynamic of reaction (1) with the specific oxygen-carrier. On the one hand, the partial pressure of O<sub>2</sub> at equilibrium conditions must be low (4 kPa or lower) at the air-reactor temperature, in order to have a high use of the oxygen in air. On the other hand, the equilibrium concentration of oxygen in the fuel-reactor will be given by the temperature in the reactor determined by the energy balance to CLOU system. A high equilibrium partial pressure of oxygen together with a very reactive oxygen-carrier will promote the overall conversion rate of the solid fuel in the fuel-reactor. In addition, the combustion of the fuel will decrease the oxygen concentration in the reactor and can improve the decomposition reaction of the metal oxide particles. The temperature at

which the air- and fuel-reactor will operate comes determined by the temperature of the incoming particles, the circulation rate, as well as the heat of reaction in both reactors, as it was analyzed by Eyring et al. for CLOU process (Eyring et al., 2011).



In the case of copper and manganese oxides, the overall reaction with carbon is exothermic in the fuel-reactor, as it is showed in reactions (8) and (9). Thus it is possible to have a temperature increase in the fuel-reactor, which results in a significantly higher partial pressure of  $O_2$  at equilibrium conditions. In the other hand the reaction of the cobalt oxide with carbon is an endothermic reaction, see reaction (10).



There are only a small number of works in the literature for CLOU process dealing with the use of Cu-, Mn-, and Co-based based materials.

Regarding the use of manganese oxides for CLOU process, several Mn-based particles supported on  $Fe_2O_3$ , NiO,  $SiO_2$  or MgO have been tested in a batch fluidized bed at Chalmers University of Technology (Azimi et al., 2011; Rydén et al., 2011b; Shulman et al., 2009, 2011). Good oxygen uncoupling and mechanical properties, as well as high reactivity with methane were showed for a Mn/Fe material after repeated redox cycles (Shulman et al., 2009). The formation of the  $Fe_xMn_{1-x}O_3$  iron manganate improves the oxygen uncoupling properties with respect to the manganese oxides. Later, the optimum molar ratio Fe:Mn was determined to be 2:1 (Azimi et al., 2011). Tests in batch fluidized bed with coal or petcoke as fuel revealed a high conversion of char, although the oxygen released was found to be around 0.5% of its initial mass. This material has

also been tested in a continuous facility with methane as fuel (Rydén et al., 2011b), showing much better oxygen uncoupling properties than a manganese ore. However, the authors pointed out that much of the synthetic particles turned into a fine dust after 4 hours of operation and collapsed material formed very soft agglomerations in the fuel-reactor.

Physical mixing of oxygen-carriers with  $\text{Mn}_2\text{O}_3$  and  $\text{Co}_3\text{O}_4$  (60 wt.%) supported on three different binders (yttria-stabilized zirconia (YSZ; 92 wt.%  $\text{ZrO}_2$  and 8wt. %  $\text{Y}_2\text{O}_3$ ),  $\text{Al}_2\text{O}_3$  and  $\text{TiO}_2$ ) were investigated with promising results on oxygen release rate (Moghtaderi, 2010). However, these materials were proposed for oxygen production in the Chemical Looping Air Separation Process (CLAS), where coal is not mixed with the oxygen-carrier.

Perovskite type materials based on Mn and Ca oxides ( $\text{CaMn}_x\text{Ti}_{1-x}\text{O}_3$ ) has also been tested in a batch fluidized facility (Leion et al., 2009c; Rydén et al., 2011a). The oxygen uncoupling properties of perovskite type materials caused a fast conversion of petcoke (Leion et al., 2009c). The perovskite material  $\text{CaMn}_{0.875}\text{Ti}_{0.125}\text{O}_3$  was later examined for 70 h in a small circulating fluidized-bed reactor using natural gas as fuel (Rydén et al., 2011a). Particles retained most of their physical properties and reactivity over the course of the experiments. In addition, high reactivity with  $\text{CH}_4$  was found, although complete conversion of natural gas was not obtained during the experimental tests.

In general, Cu-based materials have faster release of oxygen than Mn-based particles (Leion et al., 2009c). Preliminary experiments were conducted using  $\text{Al}_2\text{O}_3$  or  $\text{ZrO}_2$  as supporting materials (Leion et al., 2009b; Mattisson et al., 2009a, 2009b). The results showed the relevance of the oxygen uncoupling properties on increasing the char conversion, which was the starting point for the proposal of the CLOU process. These works were done in a batch fluidized-bed reactor, and high rate of char conversion was found for several carbonaceous materials, including petcoke, coal, and biomass (Leion et al., 2009b). It was found a 50 times increase in the conversion rate of petroleum coke at CLOU conditions with CuO relative to those measured with Fe-based oxygen-carrier in a CLC system with solid fuels (Mattisson et al., 2009a). It is noteworthy that Fe-based materials do not have oxygen uncoupling properties. A solids inventory between 120 and 200  $\text{kg/MW}_{\text{th}}$  was estimated for CLOU process using Cu-based particles, which

was much lower than the amount of solids required in a CLC system (2000 kg/MW<sub>th</sub> for Fe-based particles) (Leion et al., 2007; Mattisson et al., 2009b). However, they found some defluidization phenomena with Cu-based particles during some parts of the experiments (Mattisson et al., 2009b).

Avoiding agglomeration with Cu-based oxygen-carriers has been a major concern in the past. Thus, for CLC conditions where CuO can be reduced to Cu agglomeration is avoided by using CuO fractions lower than 20 wt.% in the particle (de Diego et al., 2005). However, the condition is different for CLOU, where CuO is reduced to Cu<sub>2</sub>O. In the research group of ICB-CSIC (Adánez-Rubio et al., 2011a; Gayán et al., 2011), a screening study considering 25 different Cu-based oxygen-carriers was done to select appropriate materials for CLOU process. Particles prepared by different methods and using several CuO contents and supporting materials were tested. Reactivity of materials was analyzed in TGA, whereas mechanical stability and fluidization properties were studied in a batch fluidized bed. Two promising Cu-based oxygen-carriers prepared by pelletizing by pressure (60 wt.% CuO supported on MgAl<sub>2</sub>O<sub>4</sub>, and 40 wt.% CuO supported on ZrO<sub>2</sub>) were selected according to their high reactivity, low attrition rate and avoidance of agglomeration during successive redox cycles by alternating nitrogen and air.

To summarize, some works using oxygen-carriers with oxygen uncoupling properties have been done mainly in batch operation mode. The oxygen uncoupling properties of carrier materials were determined by analyzing the break off of oxygen in nitrogen and the conversion of CH<sub>4</sub> or solid fuels (petcoke, coal, biomass). However, the CLOU concept is based on the use of two interconnected fluidized beds, the oxygen-carrier being continuously circulating between them. In continuously operated units, only limited information about the oxygen uncoupling properties of two Mn-based materials using a gaseous fuel (CH<sub>4</sub>) in the fuel-reactor can be found (Rydén et al., 2011a, 2011b). Up to date, no experimental evidence has been found in the literature about the CLOU concept with solid fuels in continuously operated systems.

The aim of this work was to investigate the proof of the concept of the CLOU process in a continuously operated CLOU plant using coal as fuel. In this work, particles prepared

by spray drying containing 60 wt% CuO and using MgAl<sub>2</sub>O<sub>4</sub> as supporting material were used as oxygen-carrier for the CLOU process. This is the first time that the CLOU concept is demonstrated in a system composed by two interconnected fluidized-bed reactors using a solid fuel (bituminous coal). The effect of operating conditions –such as temperature of the fuel-reactor, the solids circulation rate and the coal feeding rate– on the combustion and CO<sub>2</sub> capture efficiencies were investigated. The results obtained were analyzed and discussed in order to be useful for the scale-up of a CLOU process fuelled with coal.

## **2. Experimental section**

### **2.1. Oxygen-carrier material**

The oxygen-carrier was a Cu-based material prepared by spray drying. Oxygen-carrier particles were manufactured by VITO (Flemish Institute for Technological Research, Belgium) using MgAl<sub>2</sub>O<sub>4</sub> spinel (Baikowski, S30CR) and CuO (PANREAC, PRS) as raw materials. The CuO content was 60 wt.%. The particles were calcined 24 h at 1100 °C. The particle size of the oxygen-carrier was +0.1-0.2 mm. From now on, the oxygen-carrier was named as Cu60MgAl. Table 1 shows the main properties of this material.

The mechanical strength, determined using a Shimpo FGN-5X crushing strength apparatus, was taken as the average value of 20 measurements of the force needed to fracture a particle. The surface area of the oxygen-carrier particles was determined by the Brunauer-Emmett-Teller (BET) method in a Micromeritics ASAP-2020, whereas the pore volume was measured by Hg intrusion in a Quantachrome PoreMaster 33. The identification of crystalline chemical species was carried out by powder X-ray diffractometer Bruker AXS graphite monochromator.

The fresh material has a very low porosity and a very low superficial area. The mechanical strength of the particles after 24 h of calcination was adequate for its use in a fluidized bed. The crystalline phases found by XRD analysis were only CuO and MgAl<sub>2</sub>O<sub>4</sub>. The oxygen transport capability,  $R_{OC}$ , was calculated in a TGA as  $R_{OC} = 1-$



$m_{red}/m_{ox}$ ,  $m_{ox}$  being the mass of fully oxidized particles and  $m_{red}$  in the reduced form, i.e. when all CuO has been reduced to Cu<sub>2</sub>O.

Preliminary results showed that similar material prepared by mechanical mixing has adequate values of reactivity and oxygen transport capacity, high attrition resistance and does not have tendency to agglomerate during operation in a fluidized-bed reactor (Gayán et al., 2011b).

## 2.2. Coal fuel

The fuel was a bituminous colombian coal “El Cerrejón”. Elementary and proximate analysis and low heating value of this coal were determined. The properties of this coal are shown in Table 2. The coal particle size used for this study was +200–300 µm.

Bed agglomeration problems with pipes clogging were found when “El Cerrejón” coal was fed into the system because this coal showed a high swelling behaviour. In order to avoid coal swelling and bed agglomeration, the coal was subjected to a thermal pre-treatment for pre-oxidation. Coal was heated at 180 °C in air atmosphere for 28 hours (Pis et al., 1996). Proximate and ultimate analyses of the pre-treated coal are shown in Table 2. The pre-oxidation causes an increase in the oxygen content from 7.2 to 17.6% and a decrease in the heating value. Despite the decrease in the heating value, the swelling properties of this coal were eliminated and agglomeration problems were not observed in any experiment carried out with this pre-treated coal.

## 2.3. Experimental set-up ICB-CSIC-s1

A schematic view of the experimental set-up used is shown in Fig. 3. The set-up was basically composed of two interconnected fluidized-bed reactors –the air- and fuel-reactors– joined by a loop seal and a riser for solids transport from the air-reactor to the fuel-reactor, a cyclone and a solids valve to control the solids circulation flow rate in the system. The reactors operate slightly higher than atmospheric pressure, taking into consideration the pressure drops in the bed and pipes to stack. The fuel-reactor (1) consisted of a bubbling fluidized bed with 50 mm of inner diameter and 200 mm bed

height.  $N_2$  or  $CO_2$  can be used as fluidizing gas. The gas flow was 186  $L_N/h$ , corresponding to a gas velocity of 0.11 m/s. The minimum fluidizing velocities of the oxygen-carrier particles are 0.006 m/s for the smallest particle size and 0.023 m/s for the biggest one. The terminal velocities of the oxygen-carrier particles are 0.40 m/s and 1.45 m/s, for the smallest and biggest particles respectively.

Coal (9) was fed in by a screw feeder (10) at the bottom of the bed just above the fuel-reactor distributor plate in order to maximize the time that the fuel and volatile matter are in contact with the bed material. The screw feeder has two stages: the first one with variable speed to control the coal flow rate, and the second one has high rotating velocity to avoid coal pyrolysis inside the screw. A small  $N_2$  flow (24 L/h) is introduced at the beginning of the screw feeder to avoid any possible volatile reverse flow.

The oxygen-carrier is decomposed in the fuel-reactor, evolving gaseous oxygen to the surroundings. The oxygen burns the volatiles and char proceeding from coal pyrolysis in the fuel-reactor. Reduced oxygen-carrier particles overflowed into the air-reactor through a U-shaped fluidized bed loop seal (2) with 30 mm of inner diameter, to avoid gas mixing between fuel and air. A  $N_2$  flow of 60  $L_N/h$  was introduced in the loop seal. Preliminary experiments were carried out to observe the distribution of gas fed to the loop seal. In experimental conditions used in this work, the gas in the loop-seal was distributed approximated at 50% in each reactor (air- and fuel-reactor).

The oxidation of the carrier took place in the air-reactor (3), consisting of a bubbling fluidized bed with 80 mm of inner diameter and 100 mm bed height, and followed by a riser with 30 mm of inner diameter. The air flow was 1740  $L_N/h$  ( $u_g = 0.40$  m/s). In addition, a secondary air flow (240  $L_N/h$ ) was introduced at the top of the bubbling bed to help particle entrainment through a riser (4).  $N_2$  and unreacted  $O_2$  left the air-reactor passing through a high-efficiency cyclone (5) and a filter before the stack. The oxidized solid particles recovered by the cyclone were sent to a solids reservoir (7), setting the oxygen-carrier ready to start a new cycle. The regenerated oxygen-carrier particles returned to the fuel-reactor by gravity from the solids reservoir through a solids valve (8) which controls the flow rates of solids entering to the fuel-reactor. A diverting solids

valve (6) located below the cyclone allowed the measurement of the solids flow rates at any time. Therefore, this design allows to control and measure the solids circulation flow rate between both reactors. The ash particles from char combustion were not recovered by the cyclone and were collected in a filter down-stream. Thus, ashes were not accumulated in the system. Finally, it is worthy of consideration that leakage of gas between both reactors was avoided by the presence of the U-shaped loop seal (2) and the solids reservoir (7). Thus, the presence of oxygen in the fuel-reactor solely should come from oxygen released by reaction (5).

The total oxygen-carrier inventory in the system was around 2.0 kg, being about 0.4 kg in the fuel-reactor. The exact amount of solids in the fuel-reactor was calculated from pressure drop measurements in the reactor for each test.

CO<sub>2</sub>, CO, H<sub>2</sub>, CH<sub>4</sub>, and O<sub>2</sub> were analyzed at the outlet stream from fuel-reactor, whereas CO<sub>2</sub>, CO and O<sub>2</sub> were analyzed from the flue gases of the air-reactor. Non-dispersive infrared (NDIR) analyzers (Maihak S710/UNOR) were used for CO, CO<sub>2</sub>, and CH<sub>4</sub> concentration determination; a paramagnetic analyzer (Maihak S710/OXOR-P) was used to determine O<sub>2</sub> concentration; and a thermal conductivity detector (Maihak S710/THERMOR) was used for H<sub>2</sub> concentration determination. In some selected experiments, the tar amount present in fuel-reactor product gas was determined following the tar protocol (Simell et al., 2000), as well as higher C<sub>2</sub>, C<sub>3</sub> and C<sub>4</sub> hydrocarbons were analyzed off-line by a gas chromatography (HP5890 Serie II).

Because of heat losses, the system is not auto-thermal and is heated up by means of various independent ovens to get independent temperature control of the air-reactor, fuel-reactor, and freeboard above the bed in the fuel-reactor. During operation, temperatures in the bed and freeboard of the fuel-reactor, air-reactor bed and riser were monitored as well as the pressure drops in important locations of the system, such as the fuel-reactor bed, the air-reactor bed and the loop seal.

## 2.4. Experimental planning

Three different experimental test series were carried out using the same batch of oxygen-carrier particles. Table 3 shows a compilation of the main variables used in each test. Oxygen-carrier particles were used during 30 h of hot fluidization conditions, whereof 18 h corresponded to coal combustion.

The fuel-reactor temperature (CLOU01-CLOU04), the coal feeding rate (CLOU05-CLOU09) and the solid circulation flow rate (CLOU01 and CLOU10-CLOU12) were varied during experimental work using “El Cerrejón” coal. The temperature in the freeboard was maintained at 900 °C in all cases. The coal fed in was varied from 67 to 256 g/h, which corresponded to a thermal power of 410 to 1560 W<sub>th</sub>. N<sub>2</sub> was used as fluidizing gas in the fuel-reactor in order to improve the evaluation of experimental results. A parameter  $\phi$  was defined to calculate the stoichiometric solid circulation rate needed for combustion of each coal feeding rate. A value of  $\phi = 1$  corresponds to the stoichiometric flow of CuO to fully convert coal to CO<sub>2</sub> and H<sub>2</sub>O throughout reactions (1-4), being the CuO reduced to Cu<sub>2</sub>O. The oxygen-carrier to fuel ratio ( $\phi$ ) was defined by the following equation:

$$\phi = \frac{0.25F_{\text{CuO}}}{\Omega_{\text{coal}}\dot{m}_{\text{coal}}} \quad (11)$$

$F_{\text{CuO}}$  being the molar flow rate of CuO and  $\dot{m}_{\text{coal}}$  the mass-based flow of coal fed-in to the reactor.  $\Omega_{\text{coal}}$  is the stoichiometric mols of oxygen, as O<sub>2</sub>, needed to convert 1 kg of coal to CO<sub>2</sub> and H<sub>2</sub>O. This value was calculated from the proximate and ultimate analysis of coal, see Table 2, taking a value of  $\Omega_{\text{coal}} = 59$  mol O<sub>2</sub> per kg of coal.

$$\Omega_{\text{coal}} = \frac{1}{100} \left( \frac{f_{\text{C}}}{M_{\text{C}}} + 0.25 \frac{f_{\text{H}}}{M_{\text{H}}} + 0.5 \frac{f_{\text{N}}}{M_{\text{N}}} + \frac{f_{\text{S}}}{M_{\text{S}}} - 0.5 \frac{f_{\text{O}}}{M_{\text{O}}} \right) \quad (12)$$

Temperature in the air-reactor was maintained at 900 °C. Air flow into the air-reactor was maintained constant for all tests, always remaining in excess over the stoichiometric oxygen demanded by the fuel. The air excess ratio,  $\lambda$ , was defined by Eq. (13). Depending on the fuel flow, the value of  $\lambda$  ranged from 1.2 to 4.7.

$$\lambda = \frac{\text{Oxygen flow in air}}{\text{Oxygen demanded}} = \frac{0.21F_{\text{air}}}{\Omega_{\text{coal}} \dot{m}_{\text{coal}}} \quad (13)$$

## 2.5 Data evaluation

To analyze the confidence of the results, a mass balance to oxygen and carbon was carried out using the measurements of the analyzers from the air- and fuel- reactors. The dry basis product gas flow in the fuel-reactor,  $F_{\text{outFR}}$ , was calculated as

$$F_{\text{outFR}} = \frac{F_{\text{inFR}}}{1 - (y_{\text{CO}_2, \text{outFR}} + y_{\text{CO}, \text{outFR}} + y_{\text{H}_2, \text{outFR}} + y_{\text{CH}_4, \text{outFR}})} \quad (14)$$

$y_{i, \text{outFR}}$  being the concentration in dry basis exiting from the fuel-reactor, where  $i$  can be:  $\text{CO}_2$ ,  $\text{CO}$ ,  $\text{H}_2$  or  $\text{CH}_4$ .

The outlet air-reactor gas flow,  $F_{\text{outAR}}$ , was calculated through the introduced  $\text{N}_2$ ,  $F_{\text{N}_2, \text{AR}}$ .

$$F_{\text{outAR}} = \frac{F_{\text{N}_2, \text{AR}}}{1 - (y_{\text{O}_2, \text{outAR}} + y_{\text{CO}_2, \text{outAR}})} \quad (15)$$

Thus, the exiting flows of  $\text{O}_2$  and  $\text{CO}_2$  from the air- and fuel-reactors can be easily calculated using the actual concentration of every gas  $i$ .

$$F_{i, \text{out}} = y_{i, \text{out}} F_{\text{out}} \quad (16)$$

Notice that nitrogen is used as fluidizing agent in the fuel-reactor during experimental work, thus  $\text{CO}_2$  comes uniquely from the coal combustion. The mass balances to oxygen and carbon were found to be accurate by using the measurements of the analyzers from the air- and fuel-reactors. The mass balance to carbon can be done as:

$$f_C \cdot \dot{m}_{\text{coal}} = f_{\text{fixC}} \cdot \dot{m}_{\text{coal}} + \dot{m}_{\text{C}, \text{vol}} = M_C (F_{\text{CO}_2, \text{outFR}} + F_{\text{CO}, \text{outFR}} + F_{\text{CH}_4, \text{outFR}} + F_{\text{CO}_2, \text{outAR}}) \quad (17)$$

$f_{\text{fixC}}$  being the carbon fraction as fixed carbon in the coal, and  $\dot{m}_{\text{C}, \text{vol}}$  the mass flow of carbon contained in the volatile matter calculated as

$$\dot{m}_{\text{C}, \text{vol}} = (f_C - f_{\text{fixC}}) \dot{m}_{\text{coal}} \quad (18)$$

The elutriation of char particles from the fuel-reactor was negligible regarding the carbon balance in the system.

From the flow of CO<sub>2</sub> and O<sub>2</sub> exiting from the fuel-reactor, the rate of oxygen generation can be calculated as:

$$r_{O_2} = \frac{\left( F_{CO_2, outFR} + F_{O_2, outFR} + 0.5(F_{CO, outFR} + F_{H_2O, outFR}) - 0.5\dot{m}_{coal} \left( \frac{f_{H_2O}}{M_{H_2O}} + \frac{f_O}{M_O} \right) \right) M_{O_2}}{m_{s, FR}} \quad (19)$$

The variation of the oxygen-carrier conversion in the fuel-reactor was calculated as:

$$\Delta X_{OC} = \frac{r_{O_2} \cdot m_{s, FR}}{0.25 F_{CuO}} \quad (20)$$

The evaluation of the CLOU performance was carried out by studying the effect of the operational variables on the carbon capture efficiency, the char conversion and the combustion efficiency in the fuel-reactor.

The carbon capture efficiency,  $\eta_{CC}$ , was defined as the fraction of carbon initially present in the coal fed in which is actually at the outlet of fuel-reactor as CO<sub>2</sub>. This is the actual CO<sub>2</sub> captured in the CLOU system, the remaining is CO<sub>2</sub> exiting together with nitrogen from the air-reactor.

$$\eta_{CC} = \frac{M_C F_{CO_2, outFR}}{f_C \cdot \dot{m}_{coal}} \quad (21)$$

The carbon capture efficiency depends on the conversion of char in the fuel-reactor. The conversion of char in the fuel-reactor,  $X_{char}$ , was calculated considering the carbon contained in the coal fed remaining in the char, i. e. fixed carbon, and the carbon not converted in the fuel-reactor, which exit as CO<sub>2</sub> from the air-reactor.

$$X_{char} = \frac{f_{fixC} \cdot \dot{m}_{coal} - M_C \cdot F_{CO_2, outAR}}{f_{fixC} \cdot \dot{m}_{coal}} \quad (22)$$

The conversion of char in the fuel-reactor was related to the temperature and the mean residence time of solids in the fuel-reactor,  $\tau_{FR}$ .  $\tau_{FR}$  is calculated by the following equation:

$$\tau_{FR} = \frac{m_{s,FR}}{\dot{m}_s} \quad (23)$$

$m_{s,FR}$  being the mass of solids in the fuel-reactor and  $\dot{m}_s$  the solids circulation rate between air- and fuel-reactors.

Finally, the combustion efficiency,  $\eta_{comb}$ , is a measure of conversion of coal to  $CO_2$  and  $H_2O$  in the fuel-reactor. The combustion efficiency in the fuel-reactor is calculated as the volatile matter and char being converted in the fuel-reactor by the  $O_2$  supplied by the oxygen-carrier. The oxygen supplied by oxygen-carrier in the fuel-reactor is calculated through the flow of oxygen containing species in the fuel-reactor product gas, excepting gaseous oxygen, i. e.  $O_2$ . The oxygen demanded by volatile matter and char in the fuel-reactor is calculated as the oxygen demanded by the coal minus the oxygen from air reacting with char in the air-reactor, calculated as the flow of  $CO_2$  from the air reactor,  $F_{CO_2,AR}$ . Therefore, the combustion efficiency was calculated as:

$$\eta_{comb} = \frac{2F_{CO_2,outFR} + F_{CO,outFR} + F_{H_2O,outFR} - \left( \frac{f_{H_2O}}{M_{H_2O}} + \frac{f_O}{M_O} \right) \dot{m}_{coal}}{\frac{\Omega_{coal}}{M_O} \dot{m}_{coal} - 2F_{CO_2,outAR}} \quad (24)$$

### 3. Results

To demonstrate the proof of the concept of the CLOU process, several tests under continuous operation were carried out in the ICB-CSIC-s1 experimental unit using coal as fuel. A Cu-based material (Cu60MgAl) was used as oxygen-carrier. As previously mentioned,  $N_2$  instead  $CO_2$  was used as fluidizing gas in order to make feasible the balance of carbon in the fuel-reactor by using  $CO_2$  concentration. In other work, it was determined that the fluidization agent does not have any influence on the oxygen uncoupling behaviour of a Cu-based oxygen-carrier (Gayán et al., 2011b).

Different fuel-reactor temperatures, coal feeding rates and solid circulation flow rates were used, see Table 3. The CLOU prototype was easy to operate and control, and steady state for each operating condition was maintained for at least 60 minutes. Agglomeration or defluidization were never detected with this Cu-based oxygen-carrier during the 30 hours of hot CLOU operation, even through the particles were highly reduced in the fuel-reactor and temperature was as high as 960 °C.

The gas compositions of fuel- and air-reactors exit gases were analyzed. As an example, Fig. 4 shows the concentration of gases (dry basis) measured as a function of the operating time for test series CLOU01-CLOU04 where the fuel-reactor temperature was varied from 900 °C to 960 °C. The solids circulation rate was maintained at a mean value of 4.2 kg/h, whereas the coal feeding rate was 0.11 kg/h, corresponding to a oxygen-carrier to fuel ratio,  $\phi$ , of 1.2, as defined by equation (11). Carbon feeding started at  $t = 17$  min. Before carbon feeding, the oxygen concentration in the fuel-reactor was at equilibrium conditions at the reactor temperature. Thus, the oxygen uncoupling effect of the oxygen-carrier is showed. After carbon feeding, a short transitional period it is shown until steady state is reached. At steady state, the gas outlet concentration and temperature were maintained uniform during the whole combustion time. When temperature was varied, a transition period appeared and stable combustion was reached usually in less than 10 min.

In all cases, no CH<sub>4</sub>, CO or H<sub>2</sub> were detected in the outlet gas stream of the fuel-reactor. The possible presence of tars or light hydrocarbons (C<sub>2</sub>-C<sub>4</sub>) was also analyzed. For some experiments, tar measurements were done using tar protocol (Simell et al., 2000) at the fuel-reactor outlet stream. Tar was not detected in the fuel-reactor outlet flow, that is, no hydrocarbons heavier than C<sub>5</sub>. In addition, gas from the fuel-reactor outlet stream was collected in bags and analysed off line using a gas chromatograph. The analysis showed that there were no C<sub>2</sub>-C<sub>4</sub> hydrocarbons in the gases. Thus, CO<sub>2</sub>, H<sub>2</sub>O and O<sub>2</sub> were the only gases at the fuel-reactor outlet together with the N<sub>2</sub> introduced as fluidizing gas. It must be pointed out that small amounts of SO<sub>2</sub> and NO<sub>x</sub> were also present at the fuel-reactor gas stream, but these components were not evaluated in this work. Therefore, volatiles were fully converted into CO<sub>2</sub> and H<sub>2</sub>O in the fuel-reactor by



reaction with the oxygen released from the CuO decomposition. In addition, the oxygen release rate was high enough to supply an excess of gaseous oxygen ( $O_2$ ) exiting together with the combustion gases. In the air-reactor the  $CO_2$  and  $O_2$  concentration decreased when the temperature increased in the fuel-reactor.

The corresponding performance parameters (i.e. combustion efficiency, carbon capture efficiency and char conversion) to the tests showed in Table 3 are summarized in Table 4. Fig. 5(a), (b) and (c) show the  $O_2$  and  $CO_2$  concentration (dry basis) exiting from the fuel- and air-reactors as a function of the fuel-reactor temperature, the coal feeding rate and the solids circulation flow rate, respectively.

The effect of the fuel-reactor temperature on the  $CO_2$  and  $O_2$  concentration in the air- and fuel-reactors are shown in Fig. 5(a). On the one hand, both  $O_2$  and  $CO_2$  concentrations from the fuel-reactor slightly increased with the temperature. The oxygen concentration was slightly lower than the equilibrium concentration, likely due to  $O_2$  reaction in the freeboard with char particles or un-burnt gases. This fact was in contrast to the  $O_2$  equilibrium concentration observed when coal was not fed to the reactor ( $t < 17$  min). On the other hand,  $CO_2$  concentration in the air-reactor decreased as the fuel-reactor temperature increased. This fact indicates that the amount of char transferred to the air-reactor decreased with the fuel-reactor temperature because of the higher char combustion rates present in fuel-reactor. However, the oxygen concentration in the air-reactor decreased with the fuel-reactor temperature. This fact is evident if it is considered that in addition to the oxygen used to burn coal, which is constant, also oxygen is released from the fuel-reactor. The decrease observed in  $O_2$  concentration from the air-reactor was due to a higher gaseous oxygen release in the fuel-reactor when increasing the fuel-reactor temperature.

The effects of the coal feeding rate on the concentration of gases are shown in Fig. 5(b). In this case, it is observed an important  $CO_2$  concentration increase in fuel-reactor with the coal feeding rate, and the oxygen concentration in the air-reactor decreases correspondingly to the increase in the oxygen demanded by the coal fed. The oxygen concentration in the fuel-reactor decreases as the coal feeding rate increases. Nevertheless, the oxygen-carrier shows high enough rate of oxygen generation to burn

all the coal in all cases and still gives an excess of gaseous oxygen. Thus, the oxygen-carrier reactivity did not limit the O<sub>2</sub> concentration release. Likely, the decrease in the oxygen concentration observed was due to a higher amount of oxygen reacting in the freeboard. If the oxygen concentration at the fuel-reactor outlet was constrained by the rate of oxygen generation of the oxygen-carrier, a sharp decrease in the oxygen concentration until values close to zero should be observed as the coal feeding rate was increased (Adánez-Rubio et al., 2011b).

In the last series of experiments, it was studied the effect of the solids circulation flow rate on the process performance. Solids circulation flow rates from 3.7 to 13.9 kg/h were used, corresponding to  $\phi$  values from 1.1 to 4.0, and the fuel-reactor temperature was 900 °C. The stoichiometric flow of solids to supply the oxygen needed to burn the coal was 3.5 kg/h. Thus the solids circulation rate was maintained above the stoichiometric flow of solids, although values close to the stoichiometric flow were used in test CLOU10, where the oxygen-carrier to fuel ratio was 1.1. Fig. 5(c) shows the O<sub>2</sub> and CO<sub>2</sub> concentration obtained in the fuel- and air-reactors with different solids circulation flow rates. CO<sub>2</sub> concentration in the fuel-reactor decreased with the circulation rate with the corresponding increase in the CO<sub>2</sub> concentration in the air-reactor. In spite of the low  $\phi$  ratio used in this experiment, no unburnt gases were detected. In all cases, H<sub>2</sub>O, CO<sub>2</sub> and O<sub>2</sub> were observed as the only product gases from the fuel-reactor. Minor variation in the concentration of gases was observed when the oxygen-carrier flow rates change.

Fig. 6(a), (b) and (c) show the variation of solids conversion as a function of the fuel-reactor temperature, coal feeding rate and solids circulation flow rate, respectively. The molar flow of CO<sub>2</sub> exiting from the fuel-reactor is also shown in these Figures.

Fig. 6(a) shows that the increase in the fuel-reactor temperature produced an increase in the CO<sub>2</sub> flow at the outlet of the fuel-reactor. Moreover, as higher is O<sub>2</sub> concentration and more char is burning in the fuel-reactor, the variation of solids conversion slightly increases with fuel-reactor temperature. Although, the variation of solids conversion in

the fuel-reactor was very high,  $\approx 80\%$  in all cases, there were not problems with the fluidization behaviour.

Fig. 6(b) shows the  $\text{CO}_2$  molar flow from the fuel-reactor and the oxygen-carrier conversion as a function of coal feeding rate. In all cases the ratio of oxygen-carrier to fuel is above the stoichiometric value. At these conditions, there was an excess of oxygen in the circulating solids and the coal combustion was not limited by the availability of reactant. As expected, the  $\text{CO}_2$  flow from fuel-reactor increased with the coal feeding rate because more fuel is burnt. Also, more oxygen is transferred between the two reactors, as it is indicated by the increase of the variation of solids conversion between 23 to 90 %. The highest coal feeding rate tested was 0.256 kg/h (test CLOU09). The solids inventory in the fuel-reactor at this condition was 235 kg/MW<sub>th</sub>. At this condition, oxygen-carrier particles were elutriated from the fuel-reactor because the high amount of gases generated in the bed. Nevertheless, during the short time of stable operation (about 15 min) full conversion of coal to  $\text{CO}_2$  and  $\text{H}_2\text{O}$  was observed, unburnt gases were not detected and there was an excess of  $\text{O}_2$  present. Unfortunately, the growth up of gas velocity in the bed prevented to work with larger coal feeding rates, although the Cu60MgAl oxygen-carrier would be able to supply the oxygen demanded by coal.

Fig. 7 shows the rate of oxygen generation, defined in Eq. (19), by Cu60MgAl oxygen-carrier as a function of the coal feeding rate, corresponding to the flows of  $\text{CO}_2$ ,  $\text{H}_2\text{O}$  and  $\text{O}_2$  exiting from the fuel-reactor. It can be seen that the oxygen transferred increases proportionally to the increase in the coal feeding rate. The upper limit for the oxygen generation rate using Cu60MgAl oxygen-carrier was not reached in the CLOU facility, although a low solid inventory was used (235 kg/MW<sub>th</sub>). This confirms the statement made that in this system the oxygen evolved in the fuel-reactor is not limited by the reaction rate of oxygen-carrier, but for the demand of oxygen by coal.

As a consequence, limited effect on the oxygen generation rate, i.e. the sum of  $\text{O}_2$  and  $\text{CO}_2$  flows, was observed when the temperature or the solids circulation flow rate (Fig. 6(c)) was varied, even though the variation of the solids conversion was as high as 0.92.

Thus, high reactivity of the oxygen-carrier was found in a wide range of variation of the solids conversion.

Fig. 8(a), (b) and (c) show the carbon capture efficiency, char conversion and the combustion efficiency as a function of the fuel-reactor temperature, the coal feeding rate and the solids circulation flow rate. Complete combustion to CO<sub>2</sub> and H<sub>2</sub>O of the coal was observed either in the fuel-reactor or the air-reactor, i. e.  $\eta_{comb} = 100\%$ . However, the char conversion in the fuel-reactor determines the carbon capture efficiency in the CLOU system by the undesirable CO<sub>2</sub> emissions in the air-reactor outlet.

It can be seen that high values of CO<sub>2</sub> capture efficiency were obtained in all cases. It is noteworthy the positive effect of fuel-reactor temperature on the CO<sub>2</sub> capture efficiency, see Fig. 8(a). Thus, when the fuel-reactor temperature was 960 °C, 99 % of carbon in coal is captured, i.e. only 1 % of carbon is exiting in the air-reactor outlet gas stream. The reason for this high CO<sub>2</sub> capture efficiency is a fast conversion of char in the fuel-reactor by combustion with gaseous oxygen. Fig. 8(a) also shows values of char conversion above 96 %, which increases with the temperature. In that sense, the CO<sub>2</sub> flow from the air-reactor decreased with the fuel-reactor temperature because more char is burned in the fuel-reactor. There is a lower char concentration in fuel-reactor due to the higher char combustion rates and a lower amount of carbon is transferred to the air-reactor.

The fuel load had not relevant effect on the CO<sub>2</sub> capture efficiency; see Fig. 8(b). Since the circulation rate and the temperature are kept constant and there is an oxygen excess in all cases, the resulting CO<sub>2</sub> capture efficiency for the different coal feeding rates does not change substantially. Thus, at the conditions used in the CLOU system, the oxygen generated in the fuel-reactor was not limited by the reactivity of this oxygen-carrier, i.e. the more oxygen is demanded, more oxygen is supplied.

Finally, Fig. 8(c) shows that an increase in the solids circulation flow causes a decrease in the char conversion and in the CO<sub>2</sub> capture efficiency. This result for CLOU with

solid fuels is opposite to the trend found for CLC with gaseous fuels, for which it was found that higher solids circulation rate leads to better performance of the system (Adánez et al., 2011). For gaseous fuels the determining factor is to have oxygen available to fully oxidize the fuel, whereas for solid fuels more factors come into consideration. The fact that there must be enough residence time for char combustion determines this resulting trend for solid fuels in this facility. Therefore, the negative effect of the solids circulation rate on the char conversion was due to the decrease in the residence time of solids in the fuel-reactor.

Both char and oxygen-carrier conversions were plotted in Fig. 9 against mean residence time in the fuel-reactor. Obviously, the greater is the residence time in the fuel-reactor, which is inversely proportional to the solids circulation flow rate, the higher are the oxygen-carrier and char conversion. A residence time above 300 s is needed to get a char conversion about 97 % at 900 °C with this coal. Notice that the mean residence time to convert a certain fraction of char will decrease when the fuel-reactor temperature increases. Thus, a char conversion of 99 % was obtained of 960 °C with a residence time of 470 s.

## **4. Discussion**

### **4.1 Operating temperature in the reactors**

The operating temperature in each reactor is a key parameter in the CLOU process, due to oxygen concentration at equilibrium condition is highly dependant on temperature.

When fuel-reactor temperature increases, carbon capture and char conversion also increase. This is due to a faster combustion rate of char at higher temperatures together with a high equilibrium partial pressure of oxygen by oxygen-carrier. Thus, an equilibrium concentration of 1.5 vol% O<sub>2</sub> can be reached in the fuel-reactor at 900 °C for CuO/Cu<sub>2</sub>O system, whereas the equilibrium concentration increases up to 12.4 vol% at 1000 °C. In addition, the consumption of oxygen by combustion of the fuel improves the decomposition reaction of the metal oxide particles.

In order to optimize the power plant efficiency it is important to keep the outlet partial pressure of  $O_2$  from the air-reactor as low as possible while combustion products are only  $CO_2$  and  $H_2O$ . This concentration will depend on the oxygen-carrier reactivity for oxidation reaction and the  $O_2$  equilibrium concentration with CuO at the actual air-reactor temperature. In the air-reactor, CuO is stable below 950 °C if the maximum oxygen concentration from the air-reactor is 4.5 vol %, whereas will be stable below 900 °C at 1.5 vol %. Thus, the use of  $O_2$  in air is higher as the temperature is lower. This is the reason for fixing the air-reactor temperature at 900 °C during the experimental work.

It is clear that the air- and fuel-reactor temperatures in the process must be adjusted according with the thermodynamic equilibrium and reaction kinetics in order to optimize the process. In fact, reaction kinetic of CuO decomposition (reaction 5) could be more relevant than the oxygen concentration at equilibrium conditions in the fuel-reactor.

The high temperature dependency of the oxygen concentration in the CLOU process makes the thermal integration between fuel-reactor and air-reactor a key aspect in the development of the technology. According to the energy balance to the CLOU system, it was thought that to reach the thermal integration in the CLOU system, the fuel-reactor temperature should be higher than air-reactor temperature (Eyring et al., 2011; Mattisson et al., 2009a). As example, Eyring et al. (Eyring et al., 2011) showed a design of a CLOU system where the air-reactor was at 850 °C and the fuel-reactor was at 950 °C. Thus, high temperatures, near 950 °C, in the fuel-reactor allow a better combustion and an increase in the carbon capture efficiency, because there is more oxygen to burn the fuel. A lower temperature in the air-reactor allows a high oxidation reaction rate. This is due to the oxidation reaction rate is carried out with the driving force of the difference between the inlet oxygen concentration (21 vol% in this case) and the oxygen concentration at equilibrium (1.5 vol%, at 900 °C). Nevertheless, in this work it has been shown that it is possible to work with both reactors, fuel- and air-reactor, at the same temperature (900 °C), keeping fuel combustion in the CLOU system. Even uncoupling behaviour was demonstrated to work at fuel-reactor temperature lower than air-reactor temperature (Gayán et al., 2011b). This fact permits to increase the degree of

freedom in the design of a CLOU system. For example, the required energy extraction from the air- and fuel-reactors can be fitted to obtain desired temperatures in both reactors.

#### **4.2 Performance of the CLOU system**

From results showed in this work during CLOU operation, char conversions from 96 to 99 % were obtained in the fuel-reactor with losses from 4 to 1 % of carbon in the air-reactor as CO<sub>2</sub>. No un-burnt gases were observed, being the combustion efficiency 100 % using Cu<sub>60</sub>MgAl as oxygen-carrier. In all CLOU tests, coal was fully converted either or in the fuel-reactor or in the air-reactor. A carbon capture of 97.5 % was reached using an oxygen-carrier inventory in the fuel-reactor of  $\approx 235$  kg/MW<sub>th</sub>. Likely, a lower inventory of solids could be used in the plant reaching also full conversion of fuel to CO<sub>2</sub> and H<sub>2</sub>O. However, at the highest coal load, the gases generated during combustion in the fuel-reactor caused an increase in the gas velocity (3-4 times the inlet velocity), which was responsible of particle elutriation from the bed. To make possible to operate at high velocity a design of the fuel-reactor as a circulating fluidized bed itself can be used.

Some gas phase oxygen was present together with the CO<sub>2</sub> stream, which should be treated in a similar way that in the exhaust gases in an oxyfuel system. It should be desirable to get low concentration of oxygen from the fuel-reactor in order to obtain a high purity CO<sub>2</sub> stream. It must be considered in the CLOU process that two different reactions take place in the fuel-reactor, namely the reaction rate of oxygen release by the oxygen-carrier and the combustion rate of the fuel, and the relation between must be considered. Thus, the CLOU system must be designed having enough amount of oxygen-carrier to release oxygen to burn the fuel, and high enough amount of solid fuel to avoid an excess of oxygen in the outlet stream from the fuel-reactor. The optimum oxygen concentration in the fuel-reactor will be a compromise between the O<sub>2</sub> generation by the oxygen-carrier and the oxygen consumption by the fuel. Thus, it has been showed in this work that increasing the coal feeding the oxygen concentration approach to zero, while the good performance of the system is not modified. This situation can be beneficial in order to obtain a CO<sub>2</sub> stream with low oxygen concentration.

A comparison between the CLOU process and the CLC with coal using Fe-based oxygen-carrier can be done. In the CLC with coal, char is gasified by steam and/or CO<sub>2</sub> in the fuel-reactor. Cuadrat et al. (Cuadrat et al., 2011) in the same ICB-CSIC-s1 facility a char conversion of 80 % and a combustion efficiency of 96 % were obtained with ilmenite inventory about 1800 kg/MW<sub>th</sub> at temperature of 950 °C. The fuel was the same Colombian coal, but ilmenite does not have oxygen uncoupling properties. So, the char was converted by steam gasification in the fuel-reactor. An oxygen polishing step has been proposed (Berguerand and Lyngfelt, 2008, 2009) to convert the un-burnt gases in the fuel-reactor outlet stream, which demands from 5 to 10 % of total oxygen required for coal combustion.

Rates of char conversion in the fuel-reactor can be used to carry out a comparison between both CLC options with solid fuels. This rate,  $(-r_C)$ , depends on the flow of carbon entering,  $F_{c,out FR}$ , and exiting,  $F_{c,in FR}$ , to and from the fuel-reactor, and the mean residence time of char particles in this reactor,  $\tau_{FR}$ . Considering the fuel-reactor as a continuous stirred tank reactor (CSTR) and a reaction rate for solid fuel conversion proportional to the char mass, the rate of char conversion was calculated as follow:

$$\frac{F_{c,out FR}}{F_{c,in FR}} = \frac{1}{(-r_C) \cdot \tau_{FR} + 1} \quad (25)$$

The flow of carbon exiting from the fuel-reactor is equal to carbon entering to air-reactor, which is emitted as CO<sub>2</sub> in the air-reactor.

Fig. 10 shows the char conversion rate calculated with this simplified model as a function of the fuel-reactor temperature with CLOU process. As expected, it can be seen that char conversion rate increase with temperature. Char conversion rates are 60 times faster than those obtained by Cuadrat et al. (Cuadrat et al., 2011) using ilmenite for Chemical-looping combustion of coal were found. Experiments carried out at 900 °C showed that the char conversion rate remained constant with increasing mean residence times of the char in the fuel-reactor.



The main reason for this important difference in the carbon capture performance between CLC with coal and CLOU is the different way which char is converted. In CLC with coal, char is converted through gasification by  $H_2O$  and/or  $CO_2$  which is slower than combustion with  $O_2$  happening in the CLOU process. As the char conversion is fast for the CLOU process, the carbon capture efficiency was high with the Colombia “El Cerrejón” coal: above 97 % in all cases, and reached 99 % at the higher temperature tested (960 °C). Nevertheless, lower values could be obtained if less reactive coals were used as fuel. If required, a system to separate chars from oxygen-carrier particles in the exiting stream of solids from the fuel-reactor could be used, e.g. a carbon stripper. Nevertheless, the amount of unconverted char recovered by the carbon stripper in the CLOU will be always lower than in CLC with coal.

Regarding the combustion efficiency, differences between CLOU and CLC with solids fuels can be due to different contact between volatile and oxidizing medium. Thus, volatiles must diffuse to emulsion phase to react with the oxygen-carrier in the CLC with solids fuels. In this case, the gas-solid contact efficiency is low. On the contrary, in the CLOU process, gaseous oxygen is evolved in emulsion, and must mix with volatiles as in common fluidized bed combustion. It seems that this process is more effective oxidizing volatile compounds.

In short, very good performance burning coal has been showed by the CLOU process. Carbon capture efficiency can be close to 100 % and full combustion of fuel to  $CO_2$  and  $H_2O$  was obtained, which avoids the need of an oxygen polishing step downstream.

## **5. Conclusions**

Coal Combustion in a continuous 1.5 kW<sub>th</sub> CLOU unit system was carried out during 18h with combustion of coal and 30h of hot fluidization operation, using an oxygen-carrier prepared by spray drying with 60 wt% of  $CuO$  and  $MgAl_2O_4$  as inert. The effect of operating conditions –such as temperature of the fuel-reactor, solids circulation rate and the coal feeding rate– on the carbon capture efficiency, and the combustion efficiency were investigated.

It was stated that no special measures must be taken because the complete combustion of fuel and high carbon capture efficiency measured. In all cases, unburnt compounds were not present in the fuel-reactor outlet, being CO<sub>2</sub> and H<sub>2</sub>O the only products of combustion even if the oxygen-carrier particles were highly converted. Thus, the CLOU process should not to require an oxygen polishing step. In all cases, oxygen was found together CO<sub>2</sub> in the gaseous stream from the fuel-reactor. The oxygen concentration from the fuel-reactor increased with the temperature. At higher fuel-reactor temperatures, the capability of Cu60MgAl particles to release oxygen is enhanced because the increase of the oxygen concentration at equilibrium conditions. To decrease the fraction of O<sub>2</sub> in the CO<sub>2</sub> stream the solid inventory must be optimized. The carbon capture efficiency depended of the fuel-reactor temperature ranging from 97 % at 900 °C to 99.3 % at 960 °C. Fast conversion of char was evidenced and increased with temperature. The rate of char conversion was as high as 27 s<sup>-1</sup> at 960 °C.

Not relevant effect on the CO<sub>2</sub> capture efficiency was observed varying the carbon feeding rate, which affect to the calculated solid inventory. Even, at the lowest solids inventory in the fuel-reactor (240 kg/MW<sub>th</sub>) full combustion of coal was observed. The maximum capability of the oxygen-carrier to produce oxygen was not reached during operation. Therefore, lower solid inventories would be needed to obtain full conversion of fuel.

An increase of solid circulation rate produced a decrease in the mean residence time of solids in the fuel-reactor, which slightly decreased the char conversion and the efficiency of carbon capture. A residence time above 300 s is needed to get a char conversion about 97 % at 900 °C with this coal.

The results obtained in this work demonstrated the proof of the concept of CLOU process for coal combustion using a Cu-based oxygen-carrier and important conclusions for the scale-up of the CLOU process were obtained.

## Acknowledgement

This work was partially supported by the European Commission, under the RFCS program (ECLAIR Project, Contract RFCP-CT-2008-0008), ALSTOM Power Boilers (France) and by the Spanish Ministry of Science and Innovation (Project ENE2010-19550). I. Adánez-Rubio thanks CSIC for the JAE fellowship.

## Nomenclature

$f_{C,fix}$	Carbon fraction as fixed carbon in the coal
$f_C$	Carbon fraction in the coal
$F_i$	Molar flow of compound i (mol/h)
$F_{in,FR}$	Dry basis gas flow introduced in the fuel-reactor (mol/s)
$f_i$	Mass fraction in coal of element or compound i.
$F_{out,AR}$	Dry basis exiting gas flow in the air-reactor (mol/s)
$F_{out,FR}$	Dry basis gas flow exiting from the fuel-reactor (mol/s)
$\dot{m}_{coal}$	Mass-based flow of coal fed-in to the fuel-reactor (kg/s)
$\dot{m}_{C,vol}$	Mass flow of carbon contained in the volatile matter (kg/s)
$M_i$	Molecular weigh of i compound (g/mol)
$\dot{m}_s$	Solids circulation rate (kg/s)
$m_{s,FR}$	Mass of solids in the fuel-reactor (kg)
$(-r_C)$	Rate of char conversion ( $s^{-1}$ )
$r_{O_2}$	Rate of oxygen generation (kg O <sub>2</sub> /s per kg of OC)
$X_{char}$	Conversion of char in the fuel-reactor
$y_i$	Molar fraction in dry basis of the i product.

## Greek letters

$\Delta H_r$	Enthalpy of reaction (kJ/mol)
$\Delta X_{OC}$	Variation of oxygen-carrier conversion

$\eta_{\text{CC}}$	Carbon capture efficiency (%)
$\eta_{\text{comb}}$	Combustion efficiency (%)
$\lambda$	Air excess ratio
$\tau_{\text{FR}}$	Mean residence time of solids in the fuel-reactor (s)
$\phi$	Oxygen-carrier to fuel ratio
$\Omega_{\text{coal}}$	Stoichiometric mols of $\text{O}_2$ to convert 1 kg of coal (mol/kg)

### Acronyms

AR	Air-reactor
CLC	Chemical-Looping Combustion
CLOU	Chemical-Looping with Oxygen Uncoupling
FR	Fuel-Reactor
in	inlet
IPCC	Intergovernmental Panel on Climate Change
OC	Oxygen-carrier
out	outlet

## References

- Adánez, J., Gayán, P., Celaya, J., de Diego, L.F., García-Labiano, F., Abad, A., 2006. Chemical looping combustion in a 10 kW<sub>th</sub> prototype using a CuO/Al<sub>2</sub>O<sub>3</sub> oxygen carrier: effect of operating conditions on methane combustion. *Ind. Eng. Chem. Res.* 45(17), 75-80.
- Adánez, J., Abad, A., García-Labiano, F., Gayán, P., de Diego, L.F., 2011. Progress in Chemical-Looping Combustion and Reforming Technologies.: A Review. *Prog. En. Comb. Sci.* doi: 10.1016/j.pecs.2011.09.001.
- Adánez-Rubio, I., Gayán, P., García-Labiano, F., de Diego, L.F., Adánez, J., Abad, A., 2011a. Development of CuO-based oxygen carrier materials suitable for chemical-looping with oxygen uncoupling (CLOU). *Energy Procedia* 4, 417-424.
- Adánez-Rubio, I., Abad, A., Gayán, P. de Diego, L.F., García-Labiano, F., Adánez, J., 2011b. Identification of Operational Regions in the Chemical-Looping with Oxygen Uncoupling (CLOU) Process with a Cu-based Oxygen-Carrier. Submitted to be published.
- Azimi, G., Leion, H., Mattisson, T., Lyngfelt, A., 2011. Chemical-looping with oxygen uncoupling using combined Mn-Fe oxides, testing in batch fluidized bed. *Energy Procedia* 4, 370-377.
- Berguerand, N., Lyngfelt, A., 2008. Design and operation of a 10 kW<sub>th</sub> chemical-looping combustor for solid fuels - Testing with South African coal. *Fuel* 87, 2713-2726.
- Berguerand, N., Lyngfelt, A., 2009. Chemical-Looping combustion of petroleum coke using ilmenite in a 10 kW<sub>th</sub> unit-High-temperature operation. *Energy Fuels* 23, 57-68.
- Cao, Y., Pan, W.P., 2006. Investigation of chemical looping combustion by solid fuels. 1. Process analysis. *Energy Fuels* 20, 57-68.
- Cuadrat, A., Abad, A., Adánez, J., de Diego, L.F., García-Labiano, F., Gayan, P. CO<sub>2</sub> Capture by Chemical-looping Coal Combustion using Ilmenite as oxygen carrier in a 500W<sub>th</sub> unit. *Proc 5<sup>th</sup> Int Conf on Clean Coal Technologies (CCT2011)*. Zaragoza, Spain; 2011.
- de Diego, L.F., Gayán, P., García-Labiano, F., Celaya, J., Abad, A., Adánez, J., 2005. Impregnated CuO/Al<sub>2</sub>O<sub>3</sub> Oxygen Carriers for Chemical-Looping Combustion: Avoiding Fluidizing Bed Agglomeration. *Energy Fuels* 19, 1850-1856.
- Eyring, E., Konya, G., Lighty, J., Sahir, A., Sarofim, A., Whitty, K., 2011. Chemical looping with copper oxide as carrier and coal as fuel. *Oil & Gas Science and Technology- Revue IFP Nouvelles Technologies* 2, 209-221.

Gayán, P., Adánez-Rubio, I., Abad, A., de Diego, L.F., García-Labiano, F., Adánez, J., 2011a. Development of CuO-based oxygen-carrier materials suitable for Chemical-Looping with Oxygen Uncoupling (CLOU) process. Submitted to be published.

Gayán, P., Adánez-Rubio, I., Abad, A., de Diego, L.F., García-Labiano, F., Adánez, J., 2011b. Evaluation of a Spray Dried CuO/MgAl<sub>2</sub>O<sub>4</sub> Oxygen-Carrier for CLOU. Submitted to be published.

HSC Chemistry 6.1® 2008. Chemical Reaction and Equilibrium Software with Thermochemical Database and Simulation Module. Outotec Research Oy.

IPCC, 2005. IPCC special report on carbon dioxide capture and storage, in: B. Metz, O. Davidson, H.C. de Coninck, M. Loos and L.A. Meyer, Editors, Working group III of the intergovernmental panel on climate change, Cambridge University.

Kerr, H.R., 2005. Capture and Separation Technology Gaps and Priority Research Needs. Carbon Dioxide Capture for Storage in Deep Geologic Formations, Elsevier Science, Amsterdam, pp. 655-660.

Kolbitsch, P., Bolhàr-Nordenkamp, J., Pröll, T., Hofbauer, H., 2009. Comparison of two Ni-based oxygen carriers for chemical looping combustion of natural gas in 140 kW continuous looping operation. *Ind. Eng. Chem. Res.* 48(11), 42-47.

Kvamsdal, H.M., Jordal, K., Bolland, O., 2007. A quantitative comparison of gas turbine cycles with CO<sub>2</sub> capture. *Energy* 32(1), 10-24.

Leion, H., Mattisson, T., Lyngfelt, A., 2007. The use of petroleum coke as fuel in chemical-looping combustion. *Fuel* 86, 1947-1958.

Leion, H., Lyngfelt, A., Johansson, M., Jerndal, E., Mattisson, T., 2008. The use of ilmenite as an oxygen carrier in chemical-looping combustion. *Chem. Eng. Res. Des.* 86, 1017-1026.

Leion, H., Mattisson, T., Lyngfelt, A., 2009a. Use of ores and industrial products as oxygen carriers in chemical-looping combustion. *Energy Fuels* 23, 2307-2315.

Leion, H., Mattisson, T., Lyngfelt, A., 2009b. Using chemical-looping with oxygen uncoupling (CLOU) for combustion of six different solid fuels. *Energy Procedia* 1, 447-453.

Leion, H., Larring, Y., Bakken, E., Bredesen, R., Mattisson, T., Lyngfelt, A., 2009c. Use of CaMn<sub>0.875</sub>Ti<sub>0.125</sub>O<sub>3</sub> as oxygen carrier in chemical looping with oxygen uncoupling. *Energy Fuels* 23, 5276-5283.

Lewis, W.K., Gilliland, E.R., 1954. Production of pure carbon dioxide. Patent 2665972.

Linderholm, C., Mattisson, T., Lyngfelt, A., 2009. Long-term integrity testing of spray-dried particles in a 10 kW chemical-looping combustor using natural gas as fuel. *Fuel* 88, 2083-2096.

Lyngfelt, A., Thunman, H., 2005. Construction and 100 h of operational experience of a 10-kW chemical-looping combustor, in: Thomas, D.C., Benson, S.M. (Eds.), Carbon dioxide capture for storage in deep geologic formations– Results from the CO<sub>2</sub> capture project, Oxford, UK: Elsevier, vol. 1, Chapter 36.

Mattisson, T., Lyngfelt, A., Leion, H., 2009a. Chemical-looping oxygen uncoupling for combustion of solid fuels. *Int. J. Greenhouse Gas Control* 3, 11-19.

Mattisson, T., Leion, H., Lyngfelt, A., 2009b. Chemical-Looping with Oxygen Uncoupling using CuO/ZrO<sub>2</sub> with petroleum coke. *Fuel* 88, 683-690.

Moghtaderi, B., 2010. Application of chemical looping concept for air separation at high temperatures. *Energy Fuel* 24, 190-198.

Pis, J.J., Centeno, T.A., Mahamund, M., Fuertes, A.B., Parra, J.B., Pajares, J.A., Bansal, R.C., 1996. Preparation of active carbons from coal part I. Oxidation of coal. *Fuel Proc. Tech.* 47, 19-38.

Pröll, T., Mayer, K., Bolhàr-Nordenkampf, J., Kolbitsch, P., Mattisson, T., Lyngfelt, A., Hofbauer, H., 2009. Natural minerals as oxygen carriers for chemical looping combustion in a dual circulating fluidized bed system. *Energy Procedia* 1, 27-34.

Rydén, M., Lyngfelt, A., Mattisson, T., 2011a. CaMn<sub>0.875</sub>Ti<sub>0.125</sub>O<sub>3</sub> as oxygen carrier for chemical oxygen combustion with oxygen uncoupling (CLOU) – Experiments in a continuously operating fluidized-bed reactor system. *Int. J. Greenhouse Gas Control* 5, 356-366.

Rydén, M., Lyngfelt, A., Mattisson, T., 2011b. Combined manganese/iron oxides as oxygen carrier for chemical-looping combustion with oxygen uncoupling (CLOU) in a circulating fluidized bed reactor system. *Energy Procedia* 4, 341-348.

Shen, L., Wu, J., Xiao, J., Song, Q., Xiao, R., 2009. Chemical-looping combustion of biomass in a 10 kW reactor with iron oxide as an oxygen carrier. *Energy Fuels* 23, 2498-2505.

Shulman, A., Cleverstam, E., Mattisson, T., Lyngfelt, A., 2009. Manganese/iron, manganese/nickel, and manganese/silicon oxides used in chemical looping with oxygen uncoupling (CLOU) for combustion of methane. *Energy Fuels* 23, 5269-5275.

Shulman, A., Cleverstam, E., Mattisson, T., Lyngfelt, A., 2011. Chemical-Looping with oxygen uncoupling using Mn/Mg-based oxygen-carriers – Oxygen release and reactivity with methane. *Fuel* 90, 941-950.

Simell, P., Stahlberg, P., Kurkela E., Albretch J., Deutch S., Sjostrom K., 2000. *Biomass and Bioenergy* 18, 19-38.

Wang, J., Anthony, E.J., 2008. Clean combustion of solid fuels. *Appl. Energy* 85, 73-79.

## Captions of figures

**Fig. 1.** Schematic diagram of the CLOU process.

**Fig. 2.** Equilibrium oxygen concentration over the CuO/Cu<sub>2</sub>O (—), Mn<sub>2</sub>O<sub>3</sub>/Mn<sub>3</sub>O<sub>4</sub> (···) and Co<sub>3</sub>O<sub>4</sub>/CoO (- - -) systems as a function of temperature.

**Fig. 3.** Schematic view of the ICB-CSIC-s1 unit for CLOU (1.5 kW<sub>th</sub>).

**Fig. 4.** Evolution of the gas composition in the air- and fuel-reactor at different fuel-reactor temperatures. Experimental tests CLOU01-CLOU04.  $\dot{m}_s = 4.2$  kg/h;  $\phi = 1.2$ . Fuel feeding to the system after vertical line,  $t = 17$  min.

**Fig. 5.** CO<sub>2</sub> and O<sub>2</sub> concentration from the fuel- and air-reactor obtained at different (a) fuel-reactor temperatures; (b) coal feeding rates; and (c) solids circulation flow rate. Fuel-reactor: CO<sub>2</sub> (--○--) and O<sub>2</sub> (--●--). Air-reactor: CO<sub>2</sub> (--Δ--) and O<sub>2</sub> (--▲--). Oxygen concentration at equilibrium in the fuel-reactor (—).

**Fig. 6.** Variation of the oxygen-carrier conversion (--Δ--) and flow of CO<sub>2</sub> exiting from the fuel-reactor (--●--) at different (a) fuel-reactor temperatures; (b) coal feeding rates; and (c) solids circulation flow rate.

**Fig. 7.** Rate of oxygen transferred by Cu<sub>60</sub>MgAl oxygen-carrier as a function of the coal feeding rate and the oxygen-carrier inventory.

**Fig. 8.** Carbon capture efficiency (--●--), char conversion (--Δ--) and combustion efficiency (▲) at different (a) fuel-reactor temperatures; (b) coal feeding rates; and (c) solids circulation flow rate.

**Fig. 9.** Variation of the oxygen-carrier conversion (--●--) and char conversion (--Δ--) as a function of the mean residence time of solids in the fuel-reactor. Experimental test series CLOU01 and CLOU10-CLOU12.  $T_{FR} = 900$  °C.

**Fig. 10.** Char conversion rate for Cu<sub>60</sub>MgAl (--●--) and ilmenite (--Δ--) as a function of fuel-reactor temperature. Data obtained with ilmenite taken from [36].



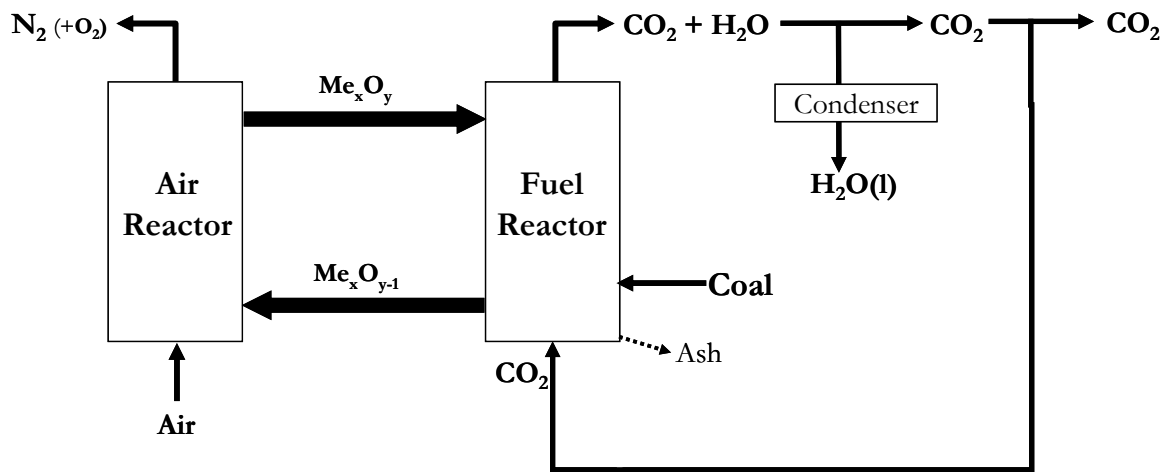


**Fig. 1.** Schematic diagram of the CLOU process.

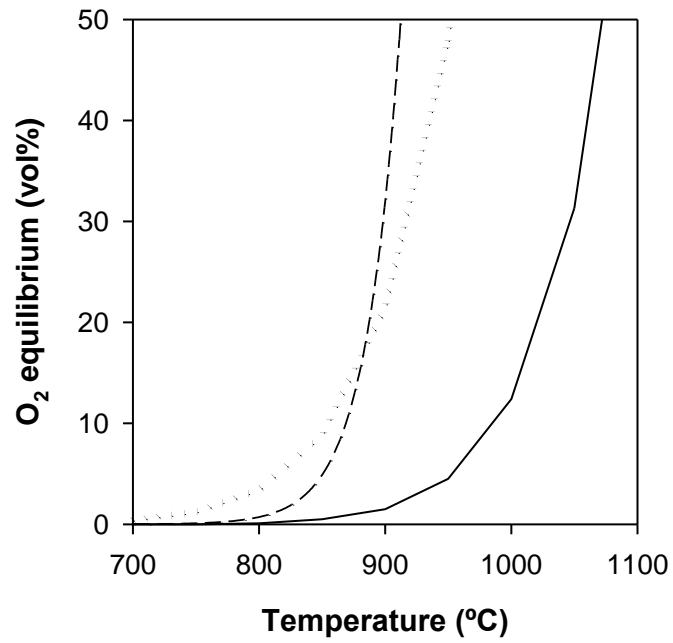


**Fig. 2.** Equilibrium oxygen concentration over the CuO/Cu<sub>2</sub>O (—), Mn<sub>2</sub>O<sub>3</sub>/Mn<sub>3</sub>O<sub>4</sub> (···) and Co<sub>3</sub>O<sub>4</sub>/CoO (- - -) systems as a function of temperature.

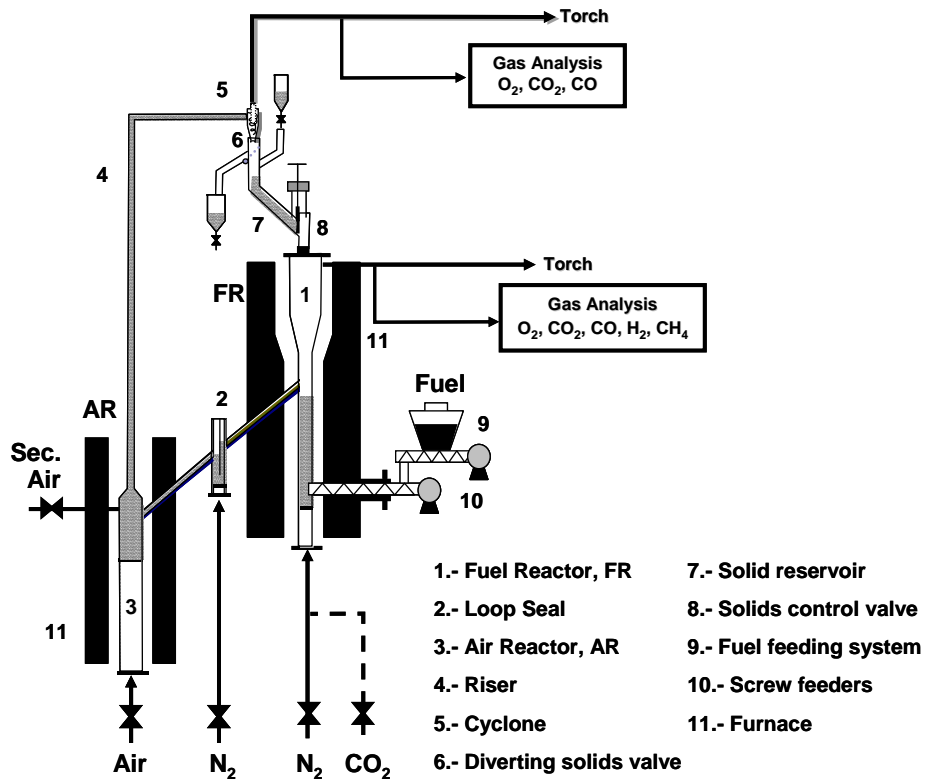


**Fig. 3.** Schematic view of the ICB-CSIC-s1 unit for CLOU (1.5 kW<sub>th</sub>).

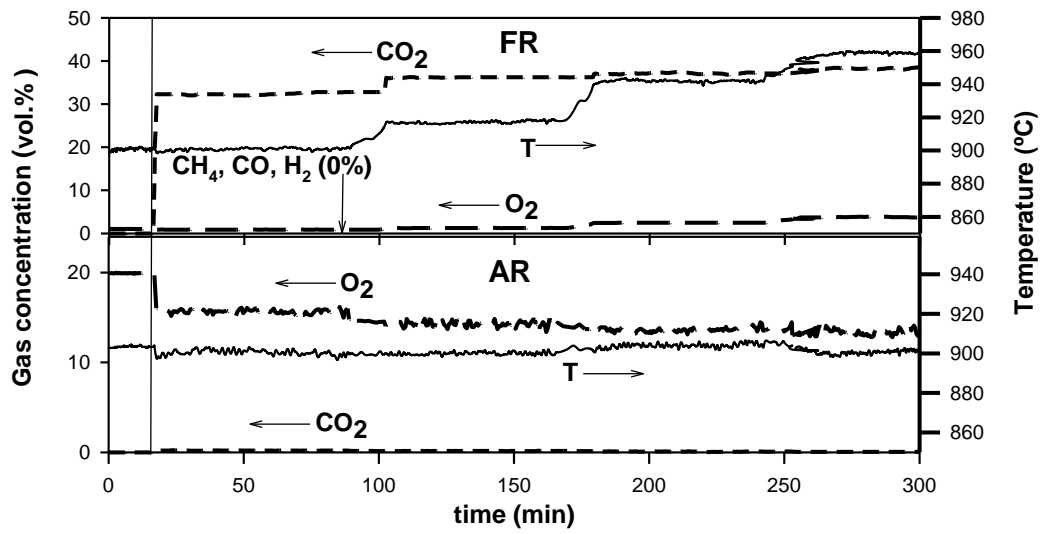


**Fig. 4.** Evolution of the gas composition in the air- and fuel-reactor at different fuel-reactor temperatures. Experimental tests CLOU01-CLOU04.  $\dot{m}_s = 4.2 \text{ kg/h}$ ;  $\phi = 1.2$ . Fuel feeding to the system after vertical line,  $t = 17 \text{ min}$ .

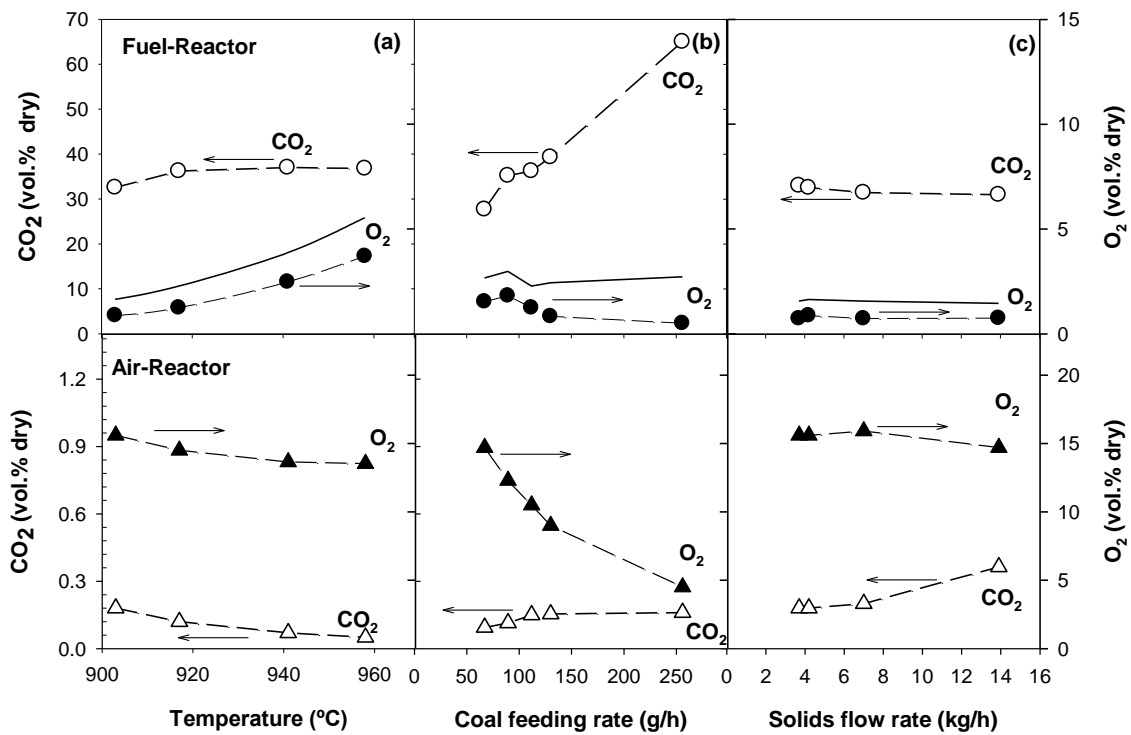


**Fig. 5.** CO<sub>2</sub> and O<sub>2</sub> concentration from the fuel- and air-reactor obtained at different (a) fuel-reactor temperatures; (b) coal feeding rates; and (c) solids circulation flow rate. Fuel-reactor: CO<sub>2</sub> (--○--) and O<sub>2</sub> (--●--). Air-reactor: CO<sub>2</sub> (--△--) and O<sub>2</sub> (--▲--). Oxygen concentration at equilibrium in the fuel-reactor (—).

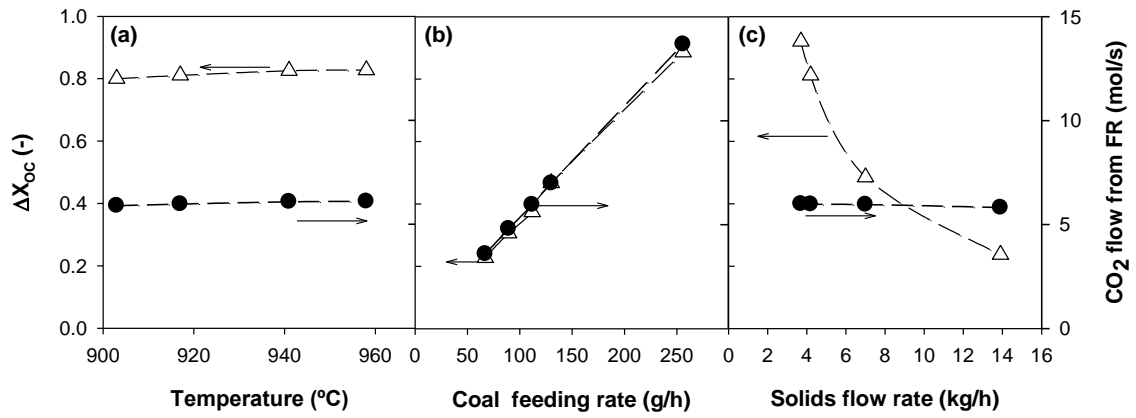


**Fig. 6.** Variation of the oxygen-carrier conversion ( $--\Delta--$ ) and flow of  $CO_2$  exiting from the fuel-reactor ( $--\bullet--$ ) at different (a) fuel-reactor temperatures; (b) coal feeding rates; and (c) solids circulation flow rate.

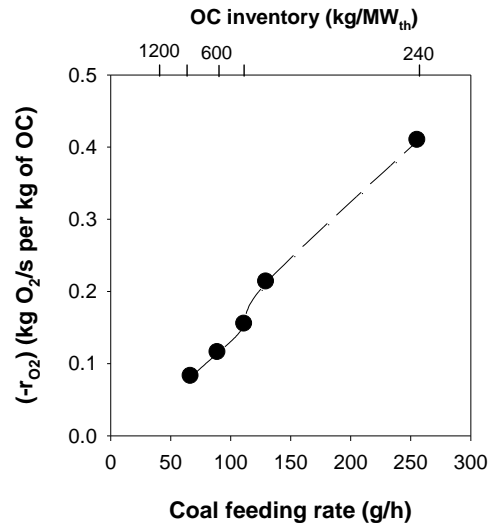


**Fig. 7.** Rate of oxygen transferred by Cu60MgAl oxygen-carrier as a function of the coal feeding rate and the oxygen-carrier inventory.

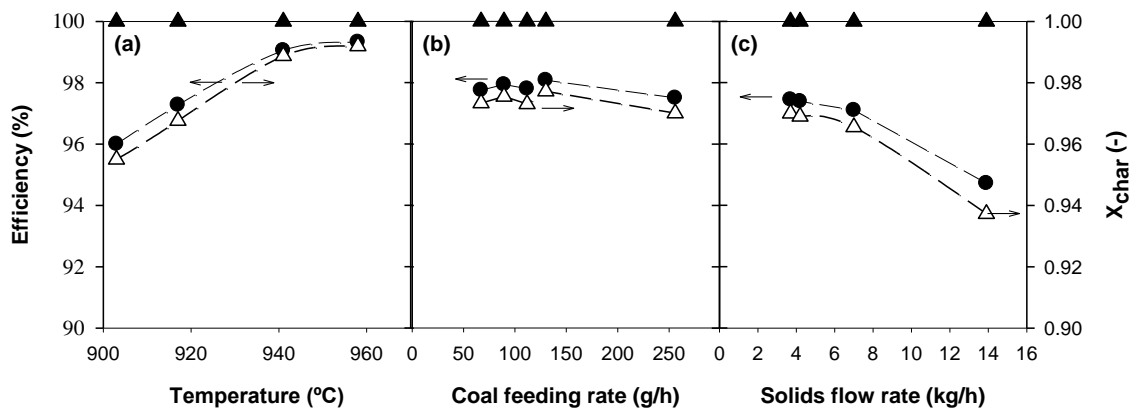


**Fig. 8.** Carbon capture efficiency ( $--\bullet--$ ), char conversion ( $--\Delta--$ ) and combustion efficiency ( $\blacktriangle$ ) at different (a) fuel-reactor temperatures; (b) coal feeding rates; and (c) solids circulation flow rate.



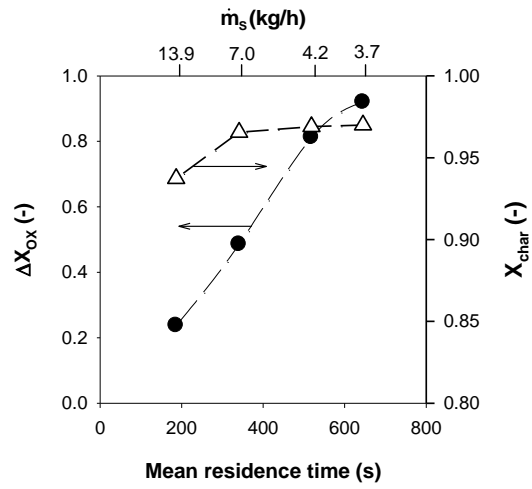


**Fig. 9.** Variation of the oxygen-carrier conversion (--●--) and char conversion (--Δ--) as a function of the mean residence time of solids in the fuel-reactor. Experimental test series CLOU01 and CLOU10-CLOU12.  $T_{FR} = 900$  °C.

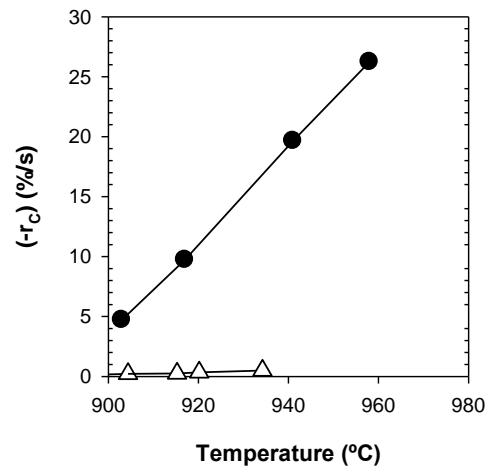


**Fig. 10.** Char conversion rate for Cu60MgAl (—●—) and ilmenite (—Δ—) as a function of fuel-reactor temperature. Data obtained with ilmenite taken from (Cuadrat et al., 2011)

## **Tables**

**Table 1.** Properties of the oxygen-carrier Cu60MgAl.

**Table 2.** Properties of fresh and pre-treated “El Cerrejón” coal.

**Table 3.** Main data for experimental tests in the continuous CLOU prototype ICB-CSIC-s1

**Table 4.** Main results for experimental tests in the continuous CLOU Prototype ICB-CSIC-s1

**Table 1.** Properties of the oxygen-carrier Cu60MgAl.

CuO content (wt%)	60
Oxygen transport capacity, $R_{OC}$ (wt%)	6
Crushing strength (N)	2.4
Real density ( $\text{kg/m}^3$ )	4600
Porosity (%)	16.1
Specific surface area, BET ( $\text{m}^2/\text{g}$ )	< 0.5
XRD main phases	CuO, $\text{MgAl}_2\text{O}_4$

**Table 2.** Properties of fresh and pre-treated “El Cerrejón” coal.

	<b>El Cerrejón</b>	
	<b>Fresh</b>	<b>Pre-treated</b>
<b>Proximate Analysis (wt.%)</b>		
Moisture	7.5 %	2.3 %
Volatile matter	34.0 %	33.0 %
Fixed carbon	49.9 %	55.9 %
Ash	8.6 %	8.8 %
<b>Ultimate Analysis (wt.%)</b>		
C	70.8 %	65.8 %
H	3.9 %	3.3 %
N	1.7 %	1.6 %
S	0.5 %	0.6 %
<b>LHV (kJ/kg)</b>	<b>25880</b>	<b>21899</b>

**Table 3.** Main data for experimental tests in the continuous CLOU Prototype ICB-CSIC-s1

Test	$T_{FR}$ (°C)	$\phi$	$\lambda$	$\dot{m}_s$ (kg/h)	$\dot{m}_{coal}$ (g/h)	Power (W)	$m_{s,FR}$ (g)	$m_{s,FR}^*$ (kg/MW <sub>th</sub> )
CLOU01	<b>903</b>	1.2	2.8	<b>4.2</b>	112	681	412	605
CLOU02	<b>917</b>	1.2	2.8	4.2	112	681	412	605
CLOU03	<b>941</b>	1.2	2.8	4.2	112	681	373	547
CLOU04	<b>960</b>	1.2	2.8	4.2	112	681	393	577
CLOU05	924	4.3	4.7	9.0	<b>67</b>	410	471	1150
CLOU06	929	3.2	3.5	9.0	<b>89</b>	541	452	835
CLOU07	917	2.6	2.8	9.0	<b>112</b>	681	412	605
CLOU08	920	2.1	2.3	9.0	<b>135</b>	821	373	454
CLOU09	925	1.1	1.2	9.0	<b>256</b>	1560	368	235
CLOU10	901	1.1	2.8	<b>3.7</b>	112	681	452	663
CLOU11	901	2.0	2.8	<b>7.0</b>	112	681	452	663
CLOU12	898	4.0	2.8	<b>13.9</b>	112	681	491	721

**Table 4.** Main results for experimental tests in the continuous CLOU Prototype ICB-CSIC-s1

Test	Combustion Efficiency	Carbon Capture Efficiency
CLOU01	100	96.0
CLOU02	100	97.3
CLOU03	100	99.1
CLOU04	100	99.3
CLOU05	100	97.8
CLOU06	100	97.9
CLOU07	100	97.8
CLOU08	100	98.1
CLOU09	100	97.5
CLOU10	100	97.5
CLOU11	100	97.1
CLOU12	100	94.7